RESEARCH ARTICLE

A Novel Output-Feedback Controller for Non-Square MIMO Nonautonomous Nonlinear Systems With Unstructured Uncertainties Using Higher-Order Switching Differentiator

JANG-HYUN PARK[ID]

Department of Electrical and Control Engineering, Mokpo National University, Muan-gun, Chonnam 58554, South Korea

e-mail: jhpark72@mokpo.ac.kr

ABSTRACT A novel output-feedback controller is proposed for multi-input multi-output (MIMO) nonautonomous nonlinear systems with unstructured uncertainties. The control system under consideration is a non-square MIMO system that may have varying numbers of control inputs and outputs. Apart from the known relative degrees of each output, the system to be controlled is completely unknown and nonautonomous. It is also assumed that the dominant control inputs for a specific system output are unknown. The proposed controller utilizes a higher-order switching differentiator (HOSD) to observe the time derivatives of composite signals that include output tracking errors. This leads to a low-complexity, approximation-free, output-feedback controller capable of compensating for unstructured uncertainties. The controller's strategy, free from universal approximators, significantly simplifies the control formula and minimizes the number of design constants. The theory shows that all output tracking errors asymptotically converge to zero. The effectiveness of the proposed controller is demonstrated through numerical simulations of three example MIMO systems.

INDEX TERMS MIMO nonlinear systems, uncertain systems, output-feedback controller, approximation-free, differentiator-based control.

I. INTRODUCTION

Conventionally, the design of stabilizing controllers for nonlinear systems characterized by unstructured uncertainties has largely leveraged sliding mode control (SMC) methods [1], [2] and adaptive control algorithms with universal approximators like neural networks (NN) or fuzzy logic systems (FLS) [3], [4], [5], [6], [7], [8], [9], [10], [11], [12], [13], [14], [15]. Although these NNs and FLS approximators have found wide application in addressing system uncertainties, they require a complex structure to ensure approximation capabilities. Furthermore, they necessitate the online updating of a multitude of adaptive parameters,

thereby leading to a heightened computational load and increased dynamic order of the controller. SMC algorithms, on the other hand, encounter certain limitations, such as the issue of chattering in control inputs and constraints on the types of nonlinear systems to which they can be effectively applied. Recently, control strategies aiming to simplify complex control formulas without compromising their performance have been proposed. This includes prescribed performance control (PPC) techniques that guarantee a predefined tracking performance irrespective of system uncertainties, and without the need for approximation [15], [16], [17], [18], [19], [20], [21]. The PPC framework significantly simplifies the controller structure by eliminating the need for universal approximators. Yet, the steps of the backstepping design continue to be an integral part of

The associate editor coordinating the review of this manuscript and approving it for publication was Xiwang Dong.

PPC methodologies, making them vulnerable to faults or large disturbances post the transient period. More recently, the proposal of differentiator-based controllers emerged, which address system uncertainties by overestimating the time-derivatives of the output tracking error, eliminating the need for universal approximations [10], [22], [23], [24], [25]. Despite the surge in research in this field, a large proportion of the studies target single-input single-output (SISO) nonlinear systems, leaving multi-input multi-output (MIMO) systems relatively under-explored.

When designing a controller for a MIMO nonlinear system with unknown dynamics, if it is discernable which input predominantly affects a specific output, the MIMO system could be decomposed into multiple single-input single-output systems, thus facilitating a simpler controller design. In general, an output is influenced by several inputs, adding complexity due to the interconnections between the inputs and outputs. Let p and q denote the number of inputs and outputs, respectively. If $p = q$, the system is referred to as fully-actuated or square. A substantial part of existing research in the control of uncertain MIMO nonlinear systems focuses on square systems (See [26], [27], [28], [29], [30], [31] and references therein). In scenarios where $p > q$, the system is classified as over-actuated, while systems where $p < q$ are considered under-actuated, with studies such as [32] and [33] dealing exclusively with this type of MIMO systems. Both of these scenarios (i.e., $p \neq q$) are collectively identified as non-square systems. The design of a versatile controller capable of being applied to both square and non-square systems is of significant importance in modern control engineering, given the prevalence of non-square structures in chemical and mechanical systems.

There are relatively few research studies that address the design of controllers for uncertain nonlinear systems that can be applied to both non-square and square cases. In [34] and [35], an adaptive fuzzy controllers for non-square nonlinear systems are proposed. The systems considered in these studies are affine-in-the-control nonlinear systems, with a multitude of FLSs utilized to estimate unknown system nonlinearities. However, stability analysis has been performed only for the over-actuated case. Similarly, [36] discusses a NN controller for non-square nonlinear systems. Nonetheless, the proposed approach has certain limitations, such as an increased complexity in the control structure due to the employment of NNs, and the restriction that the controlled system must conform to an affine form. Reference [37] presents a direct adaptive neural state-feedback control law for non-square nonlinear systems. Nevertheless, the MIMO nonlinear system under consideration consists of multiple 2nd-order affine systems, which is a fairly restrictive condition.

This paper proposes a novel approximation-free output-feedback controller for non-square nonlinear systems with unknown dynamics, based on the controller proposed in [22] and [25]. The system under consideration is significantly broader in scope than those presented in previous literature, and the proposed controller is designed to be applicable to both square and non-square nonlinear systems. The design heavily relies on higher-order switching differentiators (HOSD) [38], [39] that estimate the differentials of time-varying signals, enabling compensation for unknown functions inherent to the controlled system. The approach first involves designing q pseudo-control terms to stabilize q outputs, after which p actual control inputs are calculated as a straightforward linear combination of these pseudo-control terms. It has been proven that with such control inputs, all system outputs can be effectively stabilized. The benefits of the controller presented in this paper, when compared to existing research, can be summarized as follows:

1) It accommodates a very general MIMO non-square nonlinear system in the broadest category.
2) The proposed output-feedback control algorithm provides a unified methodology for designing control laws applicable to both non-square and square systems.
3) The structure of the controller and the process of stability proof are relatively uncomplicated due to the absence of universal approximators.

To the best of our knowledge, there are very few research findings on the design of output-feedback controllers for nonautonomous MIMO non-square nonlinear systems as general as (1). We present three simulation examples to illustrate the performance of the proposed controller and the consistency in its design.

II. PROBLEM FORMULATION
In the succeeding sections of this paper, the 2-norm of the vector $\mathbf{x}$ is represented by $|\mathbf{x}|$, and the absolute value of the scalar v is indicated by $|v|$. The notation $a(t) \rightarrow 0$ is used as an abbreviation for $\lim_{t \to \infty} a(t) = 0$, signifying that as t approaches infinity, the value of $a(t)$ converges to zero. Likewise, $a(t) \rightarrow b(t)$ is used to denote that $a(t)$ asymptotically approximates $b(t)$ as t approaches infinity, in other words, $\lim_{t \to \infty} a(t) = b(t)$.

The following nonautomonous MIMO nonlinear system is considered

$$\dot{\mathbf{x}} = \mathbf{f}(\mathbf{x}, \mathbf{u}, t)$$
$$\mathbf{y} = \mathbf{h}(\mathbf{x}, t) \qquad (1)$$

where $\mathbf{x} \in \mathbb{R}^n$ is a state vector and n is the number of state variables, $\mathbf{u} = [u_1, u_2, \cdots, u_p]^T \in \mathbb{R}^p$ is a control input vector, and $\mathbf{y} = [y_1, y_2, \cdots, y_q]^T \in \mathbb{R}^q$ is an output vector. The p and q are the numbers of inputs and outputs, respectively. The $\mathbf{f}(\cdot)$ and $\mathbf{h}(\cdot)$ are unknown smooth function vectors. The system under consideration is an exceedingly general nonlinear system, encompassing a broad range of categories such as strict- and pure-feedback systems. Most contemporary control systems fall under this category; examples include robotic arms, chemical processes, wind energy conversion systems, and car navigation systems, among others. This system also exhibits nonautonomous

characteristic since the functions $\mathbf{f}(\cdot)$ and $\mathbf{h}(\cdot)$ are explicitly time-dependent. This system taxonomy has the potential to incorporate systems with time-varying parameters and disturbances that are either additive or multiplicative. It is also assumed that only the output vector $\mathbf{y}$ is measurable. In most real-world engineering systems, all states are typically confined within certain bounded operational regions due to various constraints, and the control inputs are also limited within specific bounds due to physical restrictions.

Assumption 1: The following open set encompasses the entire operation region of the system (1)

$$\Omega = \left\{ \mathbf{x}, \mathbf{u} \middle| |\mathbf{x}| < \lambda_x, |\mathbf{u}| < \lambda_u \right\} \quad (2)$$

where λ_x and λ_u are positive bounding constants, the knowledge of which is not required.

The primary control objective is to ensure that $y_i(t)$ closely aligns with the desired output, $\psi_i(t)$, for all $i = 1, \cdots, q$, while simultaneously guaranteeing that all time-varying signals are effectively bounded. The output tracking error is defined as $z_i \triangleq y_i - \psi_i$, and its differentials w.r.t. time are derived as follows:

$$\dot{z}_i = \frac{\partial \mathbf{h}}{\partial \mathbf{x}} \mathbf{f} + \frac{\partial \mathbf{h}(\mathbf{x}, t)}{\partial t} - \dot{\psi}_i \triangleq z_{i,2}(\mathbf{x}, t)$$

$$\ddot{z}_i = \frac{\partial z_{i,2}(\mathbf{x}, t)}{\partial \mathbf{x}} \mathbf{f} + \frac{\partial z_{i,2}(\mathbf{x}, t)}{\partial t} \triangleq z_{i,3}(\mathbf{x}, t)$$

$$\vdots$$

$$z_i^{(j)} = \frac{\partial z_{i,j}(\mathbf{x}, t)}{\partial \mathbf{x}} \mathbf{f} + \frac{\partial z_{i,j}(\mathbf{x}, t)}{\partial t} \triangleq z_{i,j+1}(\mathbf{x}, t)$$

$$j = 1, \cdots, r_i - 1$$

$$\vdots$$

$$z_i^{(r_i)} = \frac{\partial z_{i,r_i}(\mathbf{x}, t)}{\partial \mathbf{x}} \mathbf{f} + \frac{\partial z_{i,r_i}(\mathbf{x}, t)}{\partial t}$$

$$\triangleq \eta_i(\mathbf{x}, \mathbf{u}, t) \quad (3)$$

for $i = 1, \cdots, q$, where r_i is the known relative degree of the y_i, that is, the minimum dynamic order in which at least one control input appears in the differential equation of $z_i^{(r_i)}$. It is assumed that the time-derivatives of the desired output $\psi_i(t)$ are bounded for all $t \geq 0$. It is noteworthy that the information about which inputs appear in the last equation of (3) is not needed for the proposed controller. In the following, the tracking error vector of y_i is denoted as $\mathbf{z}_i = [z_i, z_{i,2}, \cdots, z_{i,r_i}]^T \in \mathbb{R}^{r_i}$.

For the controllability of the system under consideration (3), the following assumption is necessary.

Assumption 2: Denote the set of indices of the inputs that appear in $\eta_i(\mathbf{x}, \mathbf{u}, t)$ as S_i. For the control gains, there exist positive constants $\lambda_{i,j}$, the knowledge of which is not required, such that

$$\frac{\partial \eta_i(\mathbf{x}, \mathbf{u}, t)}{\partial u_j} > \lambda_{i,j} \quad (4)$$

for all $j \in S_i$, $i = 1, \cdots, q$.

From Assumption 2, it can be inferred that all the control directions are assumed to be positive.

III. CONTROLLER DESIGN
A. BRIEF INTRODUCTION OF THE HOSD
In this paper, the HOSD is employed to observe the time-derivatives of composite signals, which will be defined later. To investigate the HOSD dynamics more thoroughly, we introduce a few important definitions. We denote Φ as the set of all time sequences that ascend indefinitely:

$$\Phi \triangleq \{(t_k)_{k=0}^{\infty} | t_0 = 0, t_k < t_{k+1} \forall k \in \mathbb{N}_0\} \quad (5)$$

where $\mathbb{N}_0 = \{0, 1, 2, \cdots\}$. Given a sequence $T = (t_k)$ that belongs to Φ, Ω_T represents a set of functions that have some or all t_k as points of discontinuity.

Definition 1: [39] For $T = (t_k) \in \Phi$, we define the set of functions as follows:

$$\overline{\Omega}_T^L \triangleq \left\{ f(t) \middle| f(t) \in \Omega_T, \sup_{\substack{t_k \leq t < t_{k+1} \\ \forall k \in \mathbb{N}_0}} |f(t)| \leq L < \infty \right\} \quad (6)$$

where $L > 0$ is a constant. The functions in $\overline{\Omega}_T^L$ are bounded in the piecewise sense (BPWS) below L.

Park [39] introduced the original HOSD, while modifications to its dynamics, which require only a single design constant, have been presented in another work by the same author [24]. The details are presented in the following lemma:

Lemma 1: [24] Suppose the time-derivatives of a signal $a_i(t)$ are BPWS such that $a_i^{(j)} \in \overline{\Omega}_T^{L_{i,j}^*}$ for $j = 1, 2, \cdots, r_i + 2$ where $L_{i,j}^*$s are positive constants and $T \in \Phi$. The HOSD dynamics are defined as follows

$$\left. \begin{array}{l} \dot{\alpha}_{i,j} = \beta_j L_i e_{\alpha_{i,j}} + \sigma_{i,j} \\ \dot{\sigma}_{i,j} = L_i \, \mathrm{sgn}\left(e_{\alpha_{i,j}}\right) \end{array} \right\}, j = 1, 2, \cdots, r_i \quad (7)$$

where $e_{\alpha_{i,j}} = \sigma_{i,j-1} - \alpha_{i,j}$ with $\sigma_{i,0} = a_i$. Choosing the design constants $\beta_j > 0$ for all j and $L_i > \max\{L_{i,1}^*, \cdots, L_{i,r_i}^*\}$ ensures that

$$\sigma_{i,j}(t) \rightarrow a_i^{(j)}(t), \, j = 1, 2, \cdots, r_i. \quad (8)$$

The comprehensive proof of Lemma 1 can be found in the work of [39]. In [24], the constants denoted by β_i have been proposed up to $i = 6$ as follows:

$$\beta_1 = 10, \beta_2 = 7, \beta_3 = 5.5, \beta_4 = 4.8, \beta_5 = 4.4, \beta_6 = 4.2. \quad (9)$$

To improve the HOSD's estimation capability, the sole design constant L_i in the ith HOSD equation should be increased. When compared to traditional time-derivative estimators, such as HGO [40] or HOSMD [1], HOSD has the advantage due to its asymptotic tracking performance and the absence of peaking or chattering in its estimates.

B. CONTROL INPUT FILTERING

In the process of generating the signal $a_i(t)$, which is input to the HOSD as shown in equation (7), a straightforward linear time-invariant (LTI) filter is utilized. The equations for this filter related to the ith output y_i are given as follows:

$$\dot{w}_{i,j} = -c_i w_{i,j} + w_{i,j+1}, \quad j = 1, \cdots, r_i - 1$$
$$\dot{w}_{i,r_i} = -c_i w_{i,r_i} + v_i(t) \tag{10}$$

In these equations, c_i is a positive design constant. The term $v_i(t)$ denotes a pseudo-control that stabilizes y_i and is defined as the linear combination of the actual control inputs, expressed by

$$v_i(t) \triangleq \sum_{j=1}^{p} m_{i,j} u_j \tag{11}$$

where $m_{i,j}$ are the design constant coefficients. Given the presence of the stabilizing components, $-c_i w_{i,j}$, for $j = 1, \cdots, r_i$ in equation (10), and considering that c_i is positive, it is guaranteed that the state variables $w_{i,j}$ of the LTI filter (10) are bounded. This is assured by the boundedness of all the control inputs u_j ($j = 1, \cdots, p$), as stated in Assumption 1. Now, we introduce the following lemma that is applicable under Assumption 1:

Lemma 2: Under Assumption 1, the following inequalities are satisfied:

$$|w_{i,j}| < \frac{|\mathbf{m}_i| \lambda_u}{c_i^{r_i-j+1}} \tag{12}$$

for $j = 1, \cdots, r_i$ where $\mathbf{m}_i = [m_{i,1}, m_{i,2}, \cdots, m_{i,p}]^T$. For a detailed proof of this Lemma, refer to [41].

The input signal to the HOSD of (7) is generated as

$$a_i = z_i - w_{i,1}. \tag{13}$$

Based on Lemma 1, we can derive the following equations:

$$\sigma_{i,1} = \dot{a}_i + d_{i,1}(t)$$
$$= \dot{z}_i - p_1(\mathbf{w}_i) - w_{i,2} + d_{i,1}(t) \tag{14}$$

$$\sigma_{i,2} = \ddot{a}_i + d_{i,2}(t)$$
$$= \ddot{z}_i - p_2(\mathbf{w}_i) - w_{i,3} + d_{i,2}(t) \tag{15}$$

$$\vdots$$

$$\sigma_{i,r_i-1} = a_i^{(r_i-1)} + d_{i,r_i-1}(t)$$
$$= z_i^{(r_i-1)} - p_{r_i-1}(\mathbf{w}_i) - w_{i,r_i} + d_{i,r_i-1}(t) \tag{16}$$

$$\sigma_{i,r_i} = a_i^{(r_i)} + d_{i,r_i}(t)$$
$$= z_i^{(r_i)} - p_{r_i}(\mathbf{w}_i) - v_i(t) + d_{i,r_i}(t) \tag{17}$$

where $\mathbf{w}_i \triangleq [w_{i,1}, w_{i,2}, \cdots, w_{i,r_i}]^T$, and $d_{i,j}(t)$ are the estimation errors that tend towards zero over time. The terms $p_k(\mathbf{w}_i)$, for $k = 1, \cdots, r_i$, are linear combinations of the elements of $\mathbf{w}_i$ and can be readily calculated for $k = 1, \cdots, 6$ as shown below:

$$p_1(\mathbf{w}_j) = -c_i w_{i,1} \tag{18}$$

$$p_2(\mathbf{w}_j) = c_i^2 w_{i,1} - 2c_i w_{i,2} \tag{19}$$

$$p_3(\mathbf{w}_j) = -c_i^3 w_{i,1} + 3c_i^2 w_{i,2} - 3c_i w_{i,3} \tag{20}$$

$$p_4(\mathbf{w}_j) = c_i^4 w_{i,1} - 4c_i^3 w_{i,2} + 6c_i^2 w_{i,3}$$
$$- 4c_j w_{i,4} \tag{21}$$

$$p_5(\mathbf{w}_j) = -c_i^5 w_{i,1} + 5c_i^4 w_{i,2} - 10c_i^3 w_{i,3}$$
$$+ 10c_i^2 w_{i,4} - 5c_i w_{i,5} \tag{22}$$

$$p_6(\mathbf{w}_j) = c_i^6 w_{i,1} - 6c_i^5 w_{i,2} + 15c_i^4 w_{i,3}$$
$$- 20c_i^3 w_{i,4} + 15c_i^2 w_{i,5} - 6c_i w_{i,6} \tag{23}$$

As stated in [24], the choice of c_i does not significantly affect the performance of the controller. Therefore, for simplifying the computation of the $p_k(\mathbf{w}_i)$s, c_i is commonly selected to be 1.

C. PSEUDO-CONTROL INPUT

We can use equations (14) through (16) to estimate the tracking error vector $\mathbf{z}_i$ as follows:

$$\hat{\mathbf{z}}_i = \begin{bmatrix} z_i \\ \sigma_{i,1} + p_1(\mathbf{w}_i) + w_{i,2} \\ \vdots \\ \sigma_{i,r_i-1} + p_{r_i-1}(\mathbf{w}_i) + w_{i,r_i} \end{bmatrix} \in \mathbb{R}^{r_i}. \tag{24}$$

According to Lemma 1, $\hat{\mathbf{z}}_i$ asymptotically tracks $\mathbf{z}_i$. Thus, we can assert the following equality

$$\mathbf{z}_i = \hat{\mathbf{z}}_i - \mathbf{d}_i(t) \tag{25}$$

where $\mathbf{d}_i(t) \triangleq [0, d_{i,1}(t), \cdots, d_{i,r_i-1}(t)]^T$. Taking into consideration equation (17), we can compute the pseudo-control v_i as follows:

$$v_i(t) = -\sigma_{i,r_i} - p_{r_i}(\mathbf{w}_i) - \mathbf{k}_i^T \hat{\mathbf{z}}_i \tag{26}$$

Here, $\mathbf{k}_i = [k_{i,1}, k_{i,2}, \cdots, k_{i,r_i}]^T$ is selected so that the polynomial

$$s^{r_i} + k_{i,r_i} s^{r_i-1} + \cdots + k_{i,2} s + k_{i,1} \tag{27}$$

is Hurwitz. To streamline the design process, we select the elements of the vector $\mathbf{k}_i$ to satisfy

$$(s + \kappa_i)^{r_i} = s^{r_i} + k_{i,r_i} s^{r_i-1} + \cdots + k_{i,2} s + k_{i,1} \tag{28}$$

where $\kappa_i > 0$. Therefore, upon choosing κ_i, we can directly compute the vector $\mathbf{k}_i$. As a result, our proposed controller only requires two design constants, $\kappa_i > 0$ in (28) and $L_i > 0$ in (7), since we typically select the design constant c_i in (10) as 1. The key result of the proposed controller is encapsulated in the following lemma:

Lemma 3: The pseudo-control input v_i defined as (26) using the HOSD (7) and input filter (10) makes the tracking error vector $\mathbf{z}_i$ asymptotically stable.

proof: Starting with (17) and (25), it is clear that the pseudo-control input (26) can be rewritten as:

$$v_i(t) = -\sigma_{i,r_i} - p_{r_i}(\mathbf{w}_i) - \mathbf{k}_i^T \hat{\mathbf{z}}_i$$
$$= -\{z_i^{(r_i)} - p_{r_i}(\mathbf{w}_i) - v_i(t) + d_{i,r_i}(t)\}$$

TABLE 1. Selected values of the matrix **G** in (36) (*p* is the number of inputs, and *q* is the number of outputs).

q \ p	1	2	3
1	1	$\begin{bmatrix} 1.1 \\ 1 \end{bmatrix}$	$\begin{bmatrix} 1.1 \\ 1 \\ 1 \end{bmatrix}$
2	$\begin{bmatrix} 1.1 & 1 \end{bmatrix}$	$\begin{bmatrix} 1.1 & 1 \\ 1 & 1.1 \end{bmatrix}$	$\begin{bmatrix} 1.1 & 1 \\ 1 & 1.1 \\ 1 & 1 \end{bmatrix}$
3	$\begin{bmatrix} 1.1 & 1 & 1 \end{bmatrix}$	$\begin{bmatrix} 1.1 & 1 & 1 \\ 1 & 1.1 & 1 \end{bmatrix}$	$\begin{bmatrix} 1.1 & 1 & 1 \\ 1 & 1.1 & 1 \\ 1 & 1 & 1.1 \end{bmatrix}$

$$- p_{r_i}(\mathbf{w}_i) - \mathbf{k}_i^T \mathbf{z}_i - \mathbf{k}_i^T \mathbf{d}_i(t)$$
$$= -z_i^{(r_i)} + v_i(t) - \mathbf{k}_i^T \mathbf{z}_i - d_{i,r_i}(t) - \mathbf{k}_i^T \mathbf{d}_i(t) \quad (29)$$

From this, we can deduce the following equality:

$$z_i^{(r_i)} = -\mathbf{k}_i^T \mathbf{z}_i + \delta_i(t) \quad (30)$$

Here, $\delta_i(t) \triangleq -d_{i,r_i}(t) - \mathbf{k}_i^T \mathbf{d}_i(t)$. In vector form, this can be expressed as

$$\dot{\mathbf{z}}_i = \mathbf{A}_i \mathbf{z}_i + \mathbf{b}_i \delta_i(t) \quad (31)$$

where

$$\mathbf{A}_i = \begin{bmatrix} 0 & 1 & 0 & \cdots & 0 \\ 0 & 0 & 1 & \cdots & 0 \\ \vdots & & & & \vdots \\ -k_{i,1} & -k_{i,2} & -k_{i,3} & \cdots & -k_{i,r_i} \end{bmatrix}, \mathbf{b}_i = \begin{bmatrix} 0 \\ 0 \\ \vdots \\ 1 \end{bmatrix}. \quad (32)$$

Positive definite matrices $\mathbf{P}_i$ and $\mathbf{Q}_i$ exist such that $\mathbf{A}_i^T \mathbf{P}_i + \mathbf{P}_i \mathbf{A}_i = -\mathbf{Q}_i$. If we define the Lyapunov function as $V_i = \mathbf{z}_i^T \mathbf{P}_i \mathbf{z}_i$, its time derivative can be expressed as

$$\dot{V}_i = -\mathbf{z}_i^T \mathbf{Q}_i \mathbf{z}_i + 2\mathbf{z}_i^T \mathbf{P}_i \mathbf{b}_i \delta_i(t)$$
$$\leq -\lambda_{min}(\mathbf{Q}_i)|\mathbf{z}_i|^2 + 2|\mathbf{z}_i|\lambda_{max}(\mathbf{P}_i)|\delta_i(t)| \quad (33)$$

where $\lambda_{min}(\cdot)$ and $\lambda_{max}(\cdot)$ are, respectively, the minimum and maximum eigenvalues of the matrix. From this inequality, it follows that if $|\mathbf{z}_i| > \zeta_i |\delta(t)|$, where $\zeta_i = \frac{2\lambda_{max}(\mathbf{P}_i)}{\lambda_{min}(\mathbf{Q}_i)}$, then $\dot{V}_i < 0$. Given that $\delta_i(t)$ asymptotically converges to zero, $|\mathbf{z}_i|$ is also asymptotically stable. ∎

D. CALCULATING REAL CONTROL INPUTS
From equations (11) and (26), we can discern the following relationship between the control input vector **u** and the pseudo-control input vector defined as $\mathbf{v} = [v_1, v_2, \cdots, v_q]^T$:

$$\mathbf{M}\mathbf{u}(t) = \mathbf{v}(t) \quad (34)$$

where

$$\mathbf{M} = \begin{bmatrix} m_{1,1} & m_{1,2} & \cdots & m_{1,p} \\ m_{2,1} & m_{2,2} & \cdots & m_{2,p} \\ \vdots & & & \vdots \\ m_{q,1} & m_{q,2} & \cdots & m_{q,p} \end{bmatrix} \in \mathbb{R}^{q \times p} \quad (35)$$

is a constant matrix. It is evident that if **M** satisfies the condition of having left pseudo-inverse matrix which is denoted as $\mathbf{G} = [g_{ij}] \in \mathbb{R}^{p \times q}$, the control input vector can be uniquely determined as

$$\mathbf{u} = \mathbf{G}\mathbf{v}. \quad (36)$$

As mentioned in the introduction, there are three possible scenarios depending on the number of inputs and outputs as follows.

1) UNDER-ACTUATED SYSTEM
In the case of $p < q$, if all the columns of **M** in (34) are independent, then **M** has left pseudoinverse matrix. To simplify the problem, the elements of **M** are chosen as given in Table 2 such that its left pseudoinverse matrix, i.e., $\mathbf{G} = (\mathbf{M}^T \mathbf{M})^{-1}\mathbf{M}^T$ becomes

$$g_{ji} = \begin{cases} 1.1, & \text{for } j = i \\ 1, & \text{for } j \neq i \end{cases} \quad (37)$$

for $i = 1, \cdots, q$, $j = 1, \cdots, p$. The rationale for this decision is to ensure that all pseudo-inputs play an almost equal role in determining a specific control input u_j. For example, if $p = 2$ and $q = 3$, the matrix **G** is determined by (37) as

$$\mathbf{G} = \begin{bmatrix} 1.1 & 1 & 1 \\ 1 & 1.1 & 1 \end{bmatrix} \quad (38)$$

which leads to

$$\begin{aligned} u_1 &= 1.1\, v_1 + v_2 + v_3 \\ u_2 &= v_1 + 1.1 v_2 + v_3 \end{aligned} \quad (39)$$

from (36).

2) OVER-ACTUATED SYSTEM
In this case, i.e., $p > q$ the $\mathbf{G} = [g_{ji}] \in \mathbb{R}^{p \times q}$ in (36) is directly chosen as defined in (37). The matrix **G** with its elements as defined in (37) evidently has its unique left pseudoinverse $\mathbf{M} = (\mathbf{G}^T \mathbf{G})^{-1}\mathbf{G}^T$ as all the columns of **G** are independent. For example, if $p = 2$ and $q = 1$, i.e., a system with 2 inputs and 1 output, the matrix **G** is chosen from Table 2 as

$$\mathbf{G} = \begin{bmatrix} 1.1 \\ 1 \end{bmatrix} \quad (40)$$

and the control input (36) is simply determined as

$$\begin{aligned} u_1 &= 1.1\, v_1 \\ u_2 &= v_1. \end{aligned} \quad (41)$$

Its left pseudo-inverse matrix **M** is calculated as

$$\mathbf{M} = (\mathbf{G}^T \mathbf{G})^{-1}\mathbf{G}^T = \begin{bmatrix} 0.49773756 & 0.45248869 \end{bmatrix} \quad (42)$$

which is also shown in Table 2 leading to

$$0.49773756 u_1 + 0.45248869 u_2 = v_1 \quad (43)$$

by (34). In the controller design, however, the matrix **M** is not used since v_is are already obtained by (26) and they

are directly fed into the LTI filters (10). Hence, v_is are not recalculated using the control inputs and $\mathbf{M}$ as in (43). The value of $\mathbf{G}$ is used only and what is crucial is the fact that it has unique left pseudoinverse matrix $\mathbf{M}$ that can reconstruct pseudo-inputs by linearly combining actual control inputs.

3) SQUARE SYSTEM

In this case, that is, $p = q$, the square matrix $\mathbf{G}$ in (36) is directly determined as (37) similar to the case of under- and over-actuated system. Therefore, the inverse matrix of $\mathbf{G}$ evidently exists, which guarantees the existence of $\mathbf{M}$ in (34). If $p = q = 2$, for example, the control inputs are determined by using $\mathbf{G} = \begin{bmatrix} 1.1 & 1 \\ 1 & 1.1 \end{bmatrix}$ and (36) as follows

$$u_1 = 1.1v_1 + v_2$$
$$u_2 = v_1 + 1.1\,v_2 \tag{44}$$

where the pseudo-control terms v_1 and v_2 are calculated using (26). As previously noted, there is no need to calculate $\mathbf{G}^{-1}(= \mathbf{M})$ as the control law only uses the elements of $\mathbf{G}$.

E. MAIN RESULT

The selected matrixes $\mathbf{G}$ for all three cases are described in Table 1 for $p = 1, 2, 3$ and $q = 1, 2, 3$. Note that if $p = q = 1$, the controlled system is SISO one in which $m_{11} = 1$ is chosen, that is, $u_1 = v_1$, which eventually becomes the control formula for the SISO system presented in [10].

The main result is described in the following theorem.

Theorem 1: Consider the system (1) under Assumption 1 and Assumption 2. The control inputs which are the linear combinations of pseudo-inputs v_i obtained by (36) make all the tracking error vectors $\mathbf{z}_i$ to be asymptotically stable.

proof: Since $\mathbf{G}$ which is chosen as (37) has a unique pseudoinverse (or inverse in square system case) matrix $\mathbf{M}$, all the pseudo-inputs of v_is can be described as a linear combinations of control inputs as (34). Because it has already proven that respective v_i which is identitical to $\sum_{j=1}^{p} m_{i,j}u_j$ stabilizes the Lyapunov function V_i asymptotically in Lemma 3, it is trivially true that linear combination of control inputs $\sum_{j=1}^{p} m_{i,j}u_j$ also drive the Lyapunov function V_i to zeros as time goes on. Therefore, it can be easily concluded that the total Lyapunov function, defined as $V = \sum_{i=1}^{q} V_i$, is also asymptotically stable. ∎

Remark 1: By introducing pseudo controls, denoted as v_i, for tracking specific system outputs and by generating the actual control inputs as linear combinations of these v_i terms, a new, streamlined control algorithm has been presented. This algorithm is designed to work effectively with both square and non-square MIMO nonlinear systems. One of the key merits of our proposed control formula is its systematic approach that remains consistent, irrespective of the type of system under consideration. Moreover, the stability analysis required for this algorithm is notably straightforward.

Remark 2: As elaborated in the introduction, the proposed output-feedback controller mitigates the impact of unstructured uncertainties in the system, delineated by equation (1),

through the overestimation of time-derivatives of the signal $a_i(t)$ up to its r_ith order, using HOSDs. This strategy not only estimates the time-derivatives of $a_i(t)$ but also approximates the unknown functions inherent to the system dynamics. As such, the necessity for employing NNs or FLSs for approximating these unknown dynamics is obviated. This elimination significantly simplifies both the control algorithm and the stability analysis. This is particularly noteworthy when compared to existing methods employing NNs or FLSs, which significantly increase the system's dynamic order and complexity due to the introduction of a multitude of tuning parameters.

IV. SIMULATIONS

In this section, the performance of the proposed output-feedback controller, as well as its design simplicity, are illustrated through three numerical simulation examples. All the following simulations have been performed using Python libraries such as NumPy, SciPy, and Matplotlib [42].

A. EXAMPLE 1

Consider the following nonlinear system, which has two inputs and two outputs [31]:

$$\dot{x}_1 = x_1 + x_2 + \frac{x_2^3}{5}$$

$$\dot{x}_2 = x_1x_2 + x_3 + u_1 + \frac{u_1^3}{7} + 0.1\cos(0.01t)\cos(x_1)$$

$$\dot{x}_3 = x_1x_2 + x_3 + u_1 + u_2 + \frac{u_2^3}{7} + 0.1\cos(0.01t)\cos(x_3)$$

$$y_1 = x_1, \ y_2 = x_3 \tag{45}$$

As observed in (45), the relative degrees of y_1 and y_2 are $r_1 = 2$ and $r_2 = 1$, respectively. The desired output for y_1 is $\psi_1(t) = \sin(t)$ and for y_2 it is $\psi_2(t) = \cos(t)$. The following LTI filters, with $c_1 = c_2 = 1$, are established for y_1:

$$\dot{w}_{1,1} = -w_{1,1} + w_{1,2}$$
$$\dot{w}_{1,2} = -w_{1,2} + v_1 \tag{46}$$

and for y_2:

$$\dot{w}_{2,1} = -w_{2,1} + v_2 \tag{47}$$

Values for v_1 and v_2 will be determined later as per (50). The following HOSD is also established for y_1:

$$\left.\begin{array}{l} e_{\alpha_{1,1}} \triangleq a_1 - \alpha_{1,1} \\ \dot{\alpha}_{1,1} = 10L_1 e_{\alpha_{1,1}} + \sigma_{1,1} \\ \dot{\sigma}_{1,1} = L_1 \operatorname{sgn}\left(e_{\alpha_{1,1}}\right) \end{array}\right\}$$

$$\left.\begin{array}{l} e_{\alpha_{1,2}} \triangleq \sigma_{1,1} - \alpha_{1,2} \\ \dot{\alpha}_{1,2} = 7L_1 e_{\alpha_{1,2}} + \sigma_{1,2} \\ \dot{\sigma}_{1,2} = L_1 \operatorname{sgn}\left(e_{\alpha_{1,2}}\right) \end{array}\right\} \tag{48}$$

and for y_2:

$$\left.\begin{array}{l} e_{\alpha_{2,1}} \triangleq a_2 - \alpha_{2,1} \\ \dot{\alpha}_{2,1} = 10L_2 e_{\alpha_{2,1}} + \sigma_{2,1} \\ \dot{\sigma}_{2,1} = L_2 \operatorname{sgn}(e_{\alpha_{2,1}}) \end{array}\right\} \tag{49}$$

TABLE 2. Calculated values of matrix M in (34).

q \ p	1	2	3
1	1	$\begin{bmatrix} 0.49773756 & 0.45248869 \end{bmatrix}$	$\begin{bmatrix} 0.34267913 & 0.31152648 & 0.31152648 \end{bmatrix}$
2	$\begin{bmatrix} 0.49773756 \\ 0.45248869 \end{bmatrix}$	$\begin{bmatrix} 5.23809524 & -4.76190476 \\ -4.76190476 & 5.23809524 \end{bmatrix}$	$\begin{bmatrix} 5.16380655 & -4.83619345 & 0.15600624 \\ -4.83619345 & 5.16380655 & 0.15600624 \end{bmatrix}$
3	$\begin{bmatrix} 0.34267913 \\ 0.31152648 \\ 0.31152648 \end{bmatrix}$	$\begin{bmatrix} 5.16380655 & -4.83619345 \\ -4.83619345 & 5.16380655 \\ 0.15600624 & 0.15600624 \end{bmatrix}$	$\begin{bmatrix} 6.77419355 & -3.22580645 & -3.22580645 \\ -3.22580645 & 6.77419355 & -3.22580645 \\ -3.22580645 & -3.22580645 & 6.77419355 \end{bmatrix}$
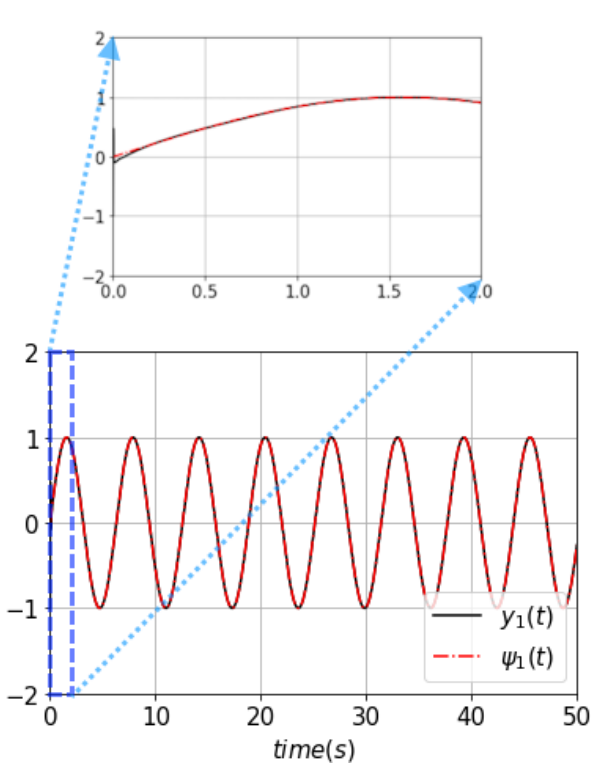
FIGURE 1. Trajectories of $y_1(t)$ and desired output $\psi_1(t)$.
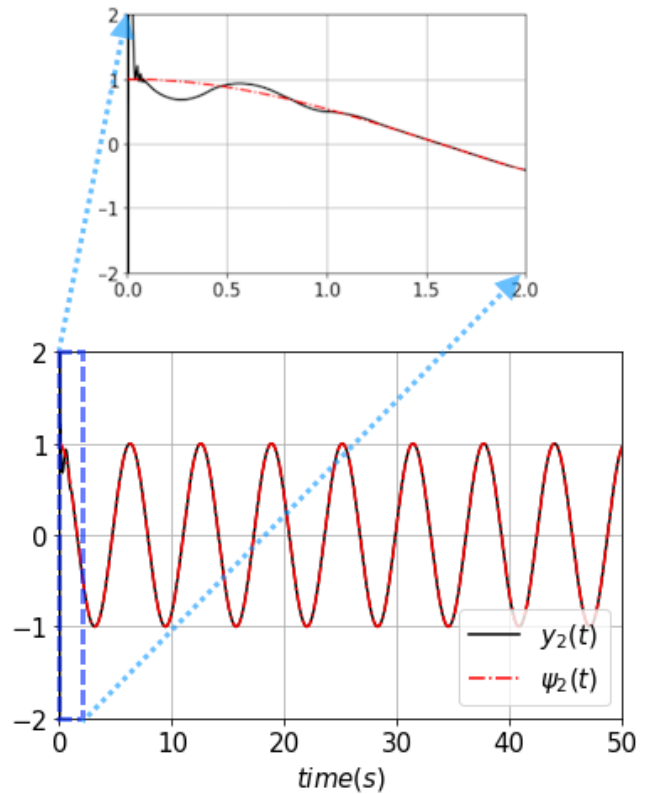
FIGURE 2. Trajectories of $y_2(t)$ and desired output $\psi_2(t)$.

where $a_1 = z_1 - w_{1,1}$ and $a_2 = z_2 - w_{2,1}$, with the constants $L_1 = L_2 = 40$ chosen. From (11), we have:

$$v_1 = -\sigma_{1,2} - p_2(w_{1,1}, w_{1,2}) - \mathbf{k_1}^T \hat{\mathbf{z}}_1$$
$$v_2 = -\sigma_{2,1} - p_1(w_{2,1}) - \kappa_2 z_2 \qquad (50)$$

where the functions $p_1(\cdot)$ and $p_2(\cdot)$ are defined as per (18) and (19), respectively. The parameters are chosen as $\kappa_1 = \kappa_2 = 20$, with $\mathbf{k}_1 = [400, 40]^T$ derived from (28). Finally, the control inputs are determined by using the matrix $\mathbf{G}$ (for the case of $p = 2, q = 2$) as shown in Table 1, and are calculated as per (39). All initial states for the LTI filters and HOSDs are set to zero. The initial states for the controlled system (45) are defined as $x_1(0) = -1$, $x_2(0) = 1$, and $x_3(0) = 0$. Simulation results are presented in Fig. 1 through Fig. 3. Figures 1 and 2

demonstrate that the system outputs track the desired outputs quite well after a brief transient period. The two control inputs are also depicted in Fig. 3.

B. EXAMPLE 2

In this section, we consider the following nonlinear system, which has three inputs and two outputs [34]:

$$\dot{x}_1 = x_2$$
$$\dot{x}_2 = x_1 + x_2^2 + x_3 + 3u_1 + u_2 + u_3 + 0.5\sin(t)$$
$$\dot{x}_3 = x_1 + 2x_2 + 3x_3x_1 + u_1 + 2(2 + 0.5\sin(x_1))u_2$$
$$\qquad + 2\sin(x_1)u_3 + 0.5\sin(t)$$
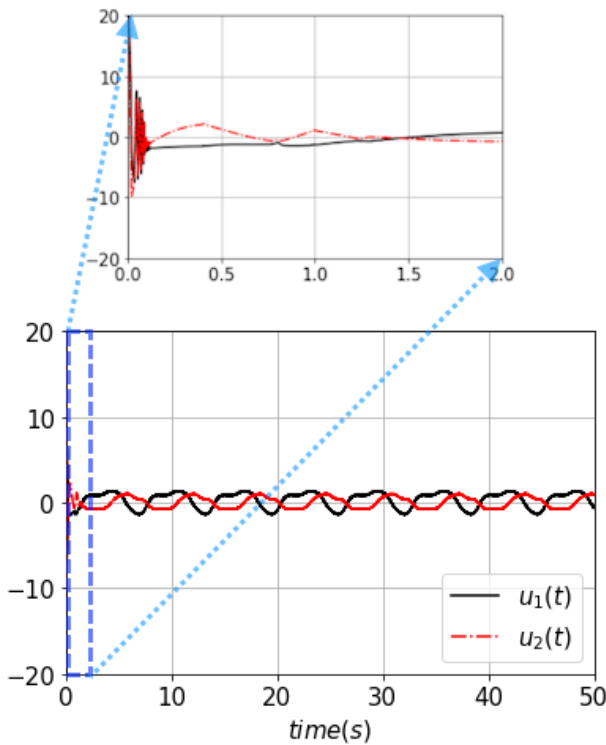$$y_1 = x_1, \ y_2 = x_3 \qquad (51)$$

FIGURE 3. Trajectories of control inputs $u_1(t)$ and $u_2(t)$.

The desired outputs are $\psi_1 = \frac{\pi}{30} \sin(t)$ and $\psi_2 = \frac{\pi}{30} \cos(t)$. As observed in (51), the relative degrees of y_1 and y_2 are $r_1 = 2$ and $r_2 = 1$, respectively. Consequently, LTI filters (46), (47) and HOSDs (48),(49) are identical to those in the previous example. The design parameters are set to $c_1 = c_2 = 1, L_1 = L_2 = 100$, and $\kappa_1 = \kappa_2 = 10$. Thus, $\mathbf{k}_1 = [100, 20]^T$ can easily be derived from (28). The matrix $\mathbf{G}$ is selected from Table 1 as follows:

$$\mathbf{G} = \begin{bmatrix} 1.1 & 1 \\ 1, & 1.1 \\ 1 & 1 \end{bmatrix} \tag{52}$$

This results in:

$$u_1 = 1.1v_1 + v_2$$
$$u_2 = v_1 + 1.1 v_2$$
$$u_3 = v_1 + v_2 \tag{53}$$

All initial states of the LTI filters and HOSDs are set to zero, as before. The initial states of the controlled system (45) are $x_1(0) = 0.1$, $x_2(0) = 0.1$, and $x_3(0) = 1$.

Simulation results are shown in Figures 4 through 6. Figures 4 and 5 illustrate that the system outputs converge to the desired outputs effectively after a brief transient period. All three control inputs are depicted in Figure 6.

C. EXAMPLE 3

Consider a ball-and-beam system as depicted in Fig. 7. Its dynamics are described as follows [33]:
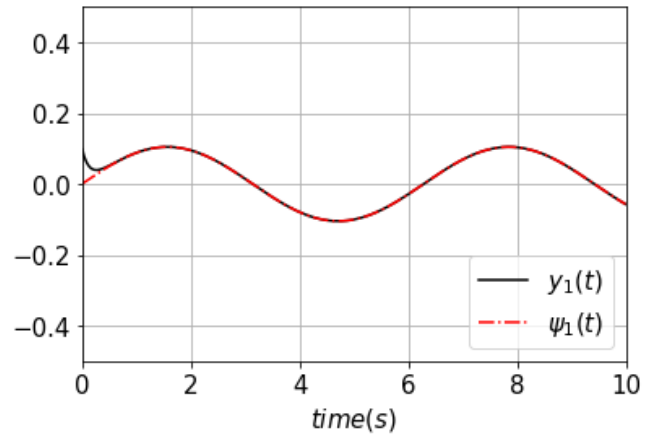
$$\dot{x}_1 = x_2$$

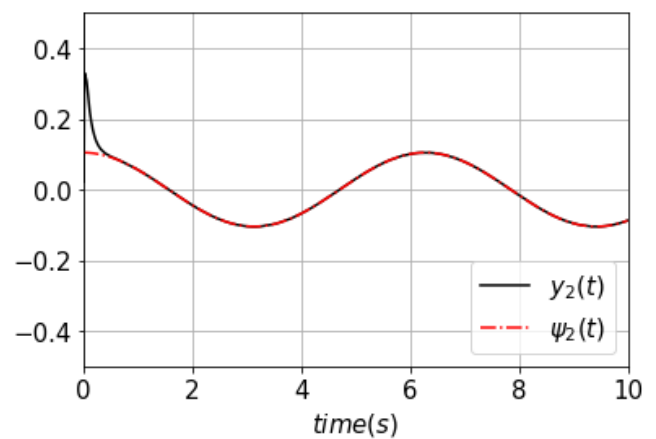**FIGURE 4.** Trajectories of $y_1(t)$ and desired output $\psi_1(t)$.

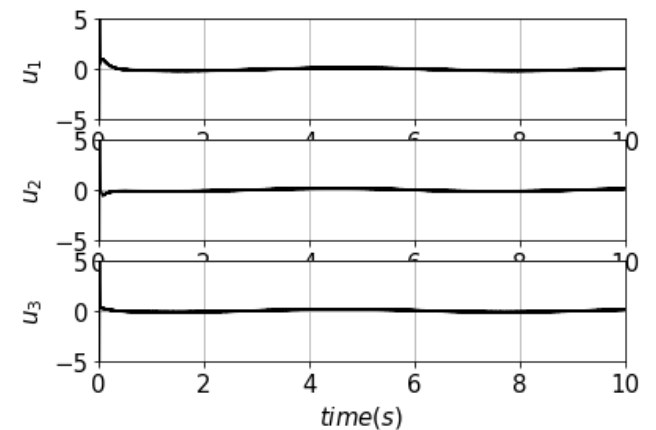**FIGURE 5.** Trajectories of $y_2(t)$ and desired output $\psi_2(t)$.

FIGURE 6. Trajectories of control inputs $u_1(t)$, $u_2(t)$, and $u_3(t)$.

$$\dot{x}_2 = u$$
$$\dot{x}_3 = x_4$$
$$\dot{x}_4 = B(x_3 x_2^2 - 9.8 \sin(x_1)) \tag{54}$$

Here, x_1 is the angle of the beam with respect to the horizontal axis, x_2 is the angular velocity of the beam, x_3 is the position
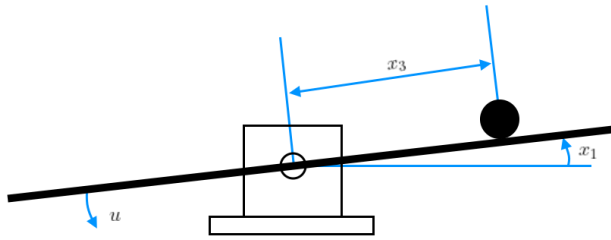
FIGURE 7. ball-and-beam system.

of the ball, and x_4 is the velocity of the ball. The constant B, used in the simulation, is set to 0.7143. The control objective is to regulate $y_1 = x_1$ and $y_2 = x_3$ to zeros using only one control input, u. The relative degrees of the outputs y_1 and y_2 are $r_1 = 1$ and $r_2 = 3$, respectively. Therefore, we define the LTI filter and HOSD for y_1 as follows:

$$\dot{w}_{1,1} = -w_{1,1} + v_1 \tag{55}$$

$$\left.\begin{array}{l} e_{\alpha_{1,1}} \triangleq a_1 - \alpha_{1,1} \\ \dot{\alpha}_{1,1} = 10L_1 e_{\alpha_{1,1}} + \sigma_{1,1} \\ \dot{\sigma}_{1,1} = L_1 \,\mathrm{sgn}(e_{\alpha_{1,1}}) \end{array}\right\} \tag{56}$$

and those for y_2 are

$$\begin{aligned} \dot{w}_{2,1} &= -w_{2,1} + w_{2,2} \\ \dot{w}_{2,2} &= -w_{2,2} + w_{2,3} \\ \dot{w}_{2,3} &= -w_{2,3} + v_2 \end{aligned} \tag{57}$$

$$\left.\begin{array}{l} e_{\alpha_{2,1}} \triangleq a_2 - \alpha_{2,1} \\ \dot{\alpha}_{2,1} = 10L_2 e_{\alpha_{2,1}} + \sigma_{2,1} \\ \dot{\sigma}_{2,1} = L_2 \,\mathrm{sgn}(e_{\alpha_{2,1}}) \end{array}\right\}$$

$$\left.\begin{array}{l} e_{\alpha_{2,2}} \triangleq \sigma_{2,1} - \alpha_{2,2} \\ \dot{\alpha}_{2,2} = 7L_2 e_{\alpha_{2,2}} + \sigma_{2,2} \\ \dot{\sigma}_{2,2} = L_2 \,\mathrm{sgn}(e_{\alpha_{2,2}}) \end{array}\right\}$$

$$\left.\begin{array}{l} e_{\alpha_{2,3}} \triangleq \sigma_{2,2} - \alpha_{2,3} \\ \dot{\alpha}_{2,3} = 5.5\,L_2 e_{\alpha_{2,3}} + \sigma_{2,3} \\ \dot{\sigma}_{2,3} = L_2 \,\mathrm{sgn}(e_{\alpha_{2,3}}) \end{array}\right\} \tag{58}$$

In these equations, the design constants are chosen to be $L_1 = L_2 = 20$. The pseudo-inputs are determined from (11) as:

$$\begin{aligned} v_1 &= -\sigma_{1,1} - p_1(w_{1,1}) - \kappa_1 z_1 \\ v_2 &= -\sigma_{3,1} - p_3(w_{2,1}, w_{2,2}, w_{2,3}) - \mathbf{k}_2^T \hat{\mathbf{z}}_2 \end{aligned} \tag{59}$$

The values for the constants are $\kappa_1 = 40$, $\kappa_2 = 10$ ($\mathbf{k}_2 = [1000, 300, 30]^T$). The gain matrix is chosen as $\mathbf{G} = [1.1, -1]$, yielding the actual control input as:

$$u = 1.1 v_1 - v_2. \tag{60}$$

Note that the matrix $\mathbf{G}$ chosen here differs from the one in Table 1. The selection of $\mathbf{G} = [1.1, -1]$ instead of $[1.1, 1]$ was made because the control gain for y_2 is not strictly positive. All initial states of the LTI filters and HOSDs are set to zero. The initial state vector of the system is $\mathbf{x} = [\frac{\pi}{30}, 0, 0.3, 0]^T$. Simulation results are shown in Figures 8 through 10. Figures 8 and 9 demonstrate that the system
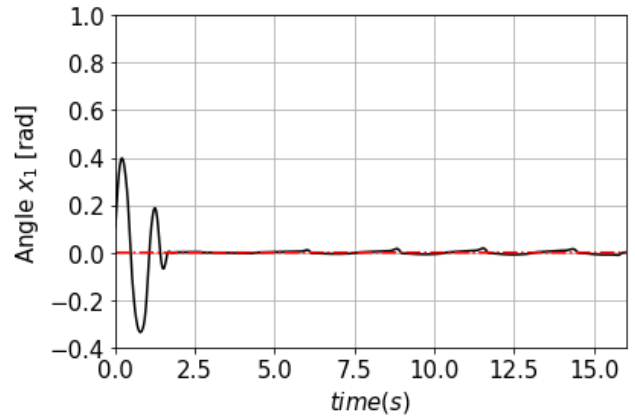

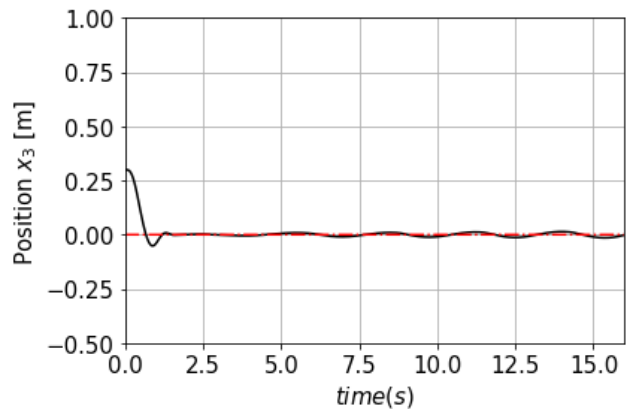**FIGURE 8. Example 3: trajectories of $y_1(= x_1)$.**

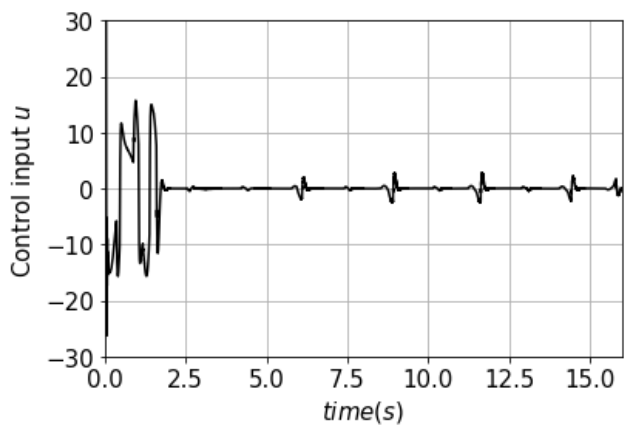**FIGURE 9. Example 3: trajectories of $y_2(= x_3)$ and desired output $\psi_2(t)$.**

FIGURE 10. Example 3: trajectories of control inputs $u(t)$.

outputs $y_1 = x_1$ and $y_2 = x_3$ are effectively regulated to zero after a short transient period. The control input u is depicted in Figure 10. These simulation results suggest that the proposed controller can be effectively applied to a system where the control direction is not strictly positive, provided the matrix $\mathbf{G}$ is appropriately chosen.

V. CONCLUSION
This paper introduces a novel output-feedback controller for MIMO nonautonomous nonlinear systems with unstructured

uncertainties. The proposed control algorithm is applicable to both square and non-square MIMO systems in a consistent manner. Despite the controlled system remaining largely unknown and nonautonomous, we assume the relative degrees of each output to be known. Furthermore, we operate under the assumption that the dominant control inputs pertaining to specific system outputs remain unknown. The controller proposed in this study employs the HOSD, enabling the monitoring of time-derivatives of compound signals composed of output tracking errors and filtered pseudo-inputs. The control inputs are computed as uncomplicated linear combinations of these pseudo-inputs. As a result, this design strategy culminates in an output-feedback controller that not only possesses minimal complexity, but also effectively compensates for unstructured uncertainties without resorting to universal approximators such as NNs or FLSs. Furthermore, the strategy significantly reduces the number of design constants. Our theoretical analysis reveals that all output tracking errors asymptotically approach zero. This finding is further substantiated by numerical simulations conducted on three representative MIMO systems, thus effectively highlighting the effectiveness of the proposed controller.

In future work, the proposed controller could be extended to systems with more relaxed conditions, such as those with unknown relative degrees or uncertain signs of input gains. It could also be applied to the design of controllers for practical MIMO systems like robotic arms or wind energy conversion systems.

REFERENCES

[1] A. Levant, "Higher-order sliding modes, differentiation and output-feedback control," *Int. J. Control*, vol. 76, nos. 9–10, pp. 924–941, Jan. 2003.

[2] A. Levant and M. Livne, "Weighted homogeneity and robustness of sliding mode control," *Automatica*, vol. 72, pp. 186–193, Oct. 2016.

[3] J.-H. Park, S.-H. Huh, S.-H. Kim, S.-J. Seo, and G.-T. Park, "Direct adaptive controller for nonaffine nonlinear systems using self-structuring neural networks," *IEEE Trans. Neural Netw.*, vol. 16, no. 2, pp. 414–422, Mar. 2005.

[4] J.-H. Park, S.-H. Kim, and C.-J. Moon, "Adaptive neural control for strict-feedback nonlinear systems without backstepping," *IEEE Trans. Neural Netw.*, vol. 20, no. 7, pp. 1204–1209, Jul. 2009.

[5] S. Tong, C. Liu, and Y. Li, "Fuzzy-adaptive decentralized output-feedback control for large-scale nonlinear systems with dynamical uncertainties," *IEEE Trans. Fuzzy Syst.*, vol. 18, no. 5, pp. 845–861, Oct. 2010.

[6] S. Cheng Tong, Y. Ming Li, and H.-G. Zhang, "Adaptive neural network decentralized backstepping output-feedback control for nonlinear large-scale systems with time delays," *IEEE Trans. Neural Netw.*, vol. 22, no. 7, pp. 1073–1086, Jul. 2011.

[7] J. Li, W. Chen, and J. Li, "Adaptive NN output-feedback decentralized stabilization for a class of large-scale stochastic nonlinear strict-feedback systems," *Int. J. Robust Nonlinear Control*, vol. 21, no. 4, pp. 452–472, Mar. 2011.

[8] S. Tong, Y. Li, and Y. Liu, "Adaptive fuzzy output feedback decentralized control of pure-feedback nonlinear large-scale systems," *Int. J. Robust Nonlinear Control*, vol. 24, no. 5, pp. 930–954, Mar. 2014.

[9] Y. Yang, D. Yue, and Y. Xue, "Decentralized adaptive neural output feedback control of a class of large-scale time-delay systems with input saturation," *J. Franklin Inst.*, vol. 352, no. 5, pp. 2129–2151, May 2015.

[10] J.-H. Park, S.-H. Kim, and T.-S. Park, "Approximation-free output-feedback control of uncertain nonlinear systems using higher-order sliding mode observer," *J. Dyn. Syst., Meas., Control*, vol. 140, no. 12, pp. 1-124502–124502-5, Dec. 2018.

[11] X. Jiang, X. Mu, and Z. Hu, "Decentralized adaptive fuzzy tracking control for a class of nonlinear uncertain interconnected systems with multiple faults and denial-of-service attack," *IEEE Trans. Fuzzy Syst.*, vol. 29, no. 10, pp. 3130–3141, Oct. 2021, doi: 10.1109/tfuzz.2020.3013700.

[12] H. Wang, P. X. Liu, J. Bao, X.-J. Xie, and S. Li, "Adaptive neural output-feedback decentralized control for large-scale nonlinear systems with stochastic disturbances," *IEEE Trans. Neural Netw. Learn. Syst.*, vol. 31, no. 3, pp. 972–983, Mar. 2020.

[13] Z. Ma and H. Ma, "Decentralized adaptive NN output-feedback fault compensation control of nonlinear switched large-scale systems with actuator dead-zones," *IEEE Trans. Syst., Man, Cybern. Syst.*, vol. 50, no. 9, pp. 3435–3447, Sep. 2020.

[14] H. Wang, B. Chen, C. Lin, and Y. Sun, "Neural-network-based decentralized output-feedback control for nonlinear large-scale delayed systems with unknown dead-zones and virtual control coefficients," *Neurocomputing*, vol. 424, pp. 255–267, Feb. 2021.

[15] S. Sui and S. Tong, "Finite-time fuzzy adaptive PPC for nonstrict-feedback nonlinear MIMO systems," *IEEE Trans. Cybern.*, vol. 53, no. 2, pp. 732–742, Feb. 2023.

[16] C. P. Bechlioulis and G. A. Rovithakis, "A low-complexity global approximation-free control scheme with prescribed performance for unknown pure feedback systems," *Automatica*, vol. 50, no. 4, pp. 1217–1226, Apr. 2014.

[17] J.-X. Zhang and G.-H. Yang, "Low-complexity tracking control of strict-feedback systems with unknown control directions," *IEEE Trans. Autom. Control*, vol. 64, no. 12, pp. 5175–5182, Dec. 2019.

[18] J.-X. Zhang, Q.-G. Wang, and W. Ding, "Global output-feedback prescribed performance control of nonlinear systems with unknown virtual control coefficients," *IEEE Trans. Autom. Control*, vol. 67, no. 12, pp. 6904–6911, Dec. 2022.

[19] Z. Guo, T. R. Oliveira, J. Guo, and Z. Wang, "Performance-guaranteed adaptive asymptotic tracking for nonlinear systems with unknown sign-switching control direction," *IEEE Trans. Autom. Control*, vol. 68, no. 2, pp. 1077–1084, Feb. 2023.

[20] S. Sui, C. L. P. Chen, and S. Tong, "A novel full errors fixed-time control for constraint nonlinear systems," *IEEE Trans. Autom. Control*, vol. 68, no. 4, pp. 2568–2575, Apr. 2023.

[21] J.-H. Park, "Output-feedback prescribed performance decentralized controller for interconnected large-scale uncertain nonlinear systems with unknown input gain sign," *IEEE Access*, vol. 11, pp. 55875–55882, 2023.

[22] J.-H. Park, T.-S. Park, and S.-H. Kim, "Approximation-free output-feedback non-backstepping controller for uncertain SISO nonautonomous nonlinear pure-feedback systems," *Mathematics*, vol. 7, no. 5, p. 456, May 2019.

[23] J.-H. Park, S.-H. Kim, and T.-S. Park, "Approximation-free state-feedback backstepping controller for uncertain pure-feedback nonautonomous nonlinear systems based on time-derivative estimator," *IEEE Access*, vol. 7, pp. 126634–126641, 2019.

[24] J.-H. Park, S.-H. Kim, and T.-S. Park, "Differentiator-based output-feedback controller for uncertain nonautonomous nonlinear systems with unknown relative degree," *IEEE Access*, vol. 8, pp. 172593–172600, 2020.

[25] J.-H. Park, S.-H. Kim, and D.-H. Lee, "Decentralized output-feedback controller for uncertain large-scale nonlinear systems using higher-order switching differentiator," *IEEE Access*, vol. 9, pp. 21227–21235, 2021.

[26] Z. Liu, X. Hu, X. Wang, and Y. Guo, "Robust adaptive control for uncertain input delay MIMO nonlinear non-minimum phase system: A fuzzy approach," *IEEE Access*, vol. 8, pp. 154143–154152, 2020, doi: 10.1109/ACCESS.2020.3018163.

[27] R. Hendel, F. Khaber, and N. Essounbouli, "Adaptive high order sliding mode controller/observer based terminal sliding mode for MIMO uncertain nonlinear system," *Int. J. Control*, vol. 94, no. 2, pp. 486–506, Feb. 2021.

[28] X. Wang, Q. Wang, and C. Sun, "Prescribed performance fault-tolerant control for uncertain nonlinear MIMO system using actor–critic learning structure," *IEEE Trans. Neural Netw. Learn. Syst.*, vol. 33, no. 9, pp. 4479–4490, Sep. 2022.

[29] J. Kong, B. Niu, Z. Wang, P. Zhao, and W. Qi, "Adaptive output-feedback neural tracking control for uncertain switched MIMO nonlinear systems with time delays," *Int. J. Syst. Sci.*, vol. 52, no. 13, pp. 2813–2830, Oct. 2021.

[30] Y. Li, K. Li, and S. Tong, "Adaptive neural network finite-time control for multi-input and multi-output nonlinear systems with positive powers of odd rational numbers," *IEEE Trans. Neural Netw. Learn. Syst.*, vol. 31, no. 7, pp. 2532–2543, Jul. 2020, doi: 10.1109/TNNLS.2019.2933409.

[31] C. He, J. Wu, J. Dai, and Z. Zhang, "Fixed-time adaptive neural tracking control for a class of uncertain multi-input and multi-output nonlinear pure-feedback systems," *Int. J. Adapt. Control Signal Process.*, vol. 35, no. 2, pp. 262–284, Feb. 2021.

[32] C.-L. Hwang, C.-C. Chiang, and Y.-W. Yeh, "Adaptive fuzzy hierarchical sliding-mode control for the trajectory tracking of uncertain underactuated nonlinear dynamic systems," *IEEE Trans. Fuzzy Syst.*, vol. 22, no. 2, pp. 286–299, Apr. 2014.

[33] F. Nafa, S. Labiod, and H. Chekireb, "Direct adaptive fuzzy sliding mode decoupling control for a class of underactuated mechanical systems," *TURKISH J. Electr. Eng. Comput. Sci.*, vol. 21, no. 6, pp. 1615–1630, 2013.

[34] S. Aloui, O. Pages, A. El Hajjaji, A. Chaari, and Y. Koubaa, "Robust fuzzy tracking control for a class of perturbed non square nonlinear systems," in *Proc. Amer. Control Conf.*, Baltimore, MD, USA, Jun. 2010, pp. 4788–4793, doi: 10.1109/acc.2010.5531116.

[35] S. Aloui, O. Pagès, A. El Hajjaji, A. Chaari, and Y. Koubaa, "Generalized fuzzy sliding mode control for MIMO nonlinear uncertain and perturbed systems," in *Proc. 18th Medit. Conf. Control Autom. MED*, Morocco, Marrakech, Jun. 2010, pp. 1164–1169.

[36] H. G. Sarand and B. Karimi, "Observer based robust neuro-adaptive control of non-square MIMO nonlinear systems with unknown dynamics," *Int. J. Comput. Intell. Syst.*, vol. 10, no. 1, pp. 23–33, 2017.

[37] K. Dheeraj, J. Jacob, and M. P. Nandakumar, "Direct adaptive neural control design for a class of nonlinear multi input multi output systems," *IEEE Access*, vol. 7, pp. 15424–15435, 2019, doi: 10.1109/ACCESS.2019.2892460.

[38] J. Park, S. Kim, and T. Park, "Asymptotically convergent switching differentiator," *Int. J. Adapt. Control Signal Process.*, vol. 33, no. 3, pp. 557–566, Mar. 2019.

[39] J.-H. Park, T.-S. Park, and S.-H. Kim, "Asymptotically convergent higher-order switching differentiator," *Mathematics*, vol. 8, no. 2, pp. 185:1–185:17, Feb. 2020.

[40] H. K. Khalil, "High-gain observers in feedback control: Application to permanent magnet synchronous motors," *IEEE Control Syst. Mag.*, vol. 37, no. 3, pp. 25–41, Jun. 2017.

[41] J.-J. E. Slotine and W. Li, *Applied Nonlinear Control*. Upper Saddle River, NJ, USA: Prentice-Hall, 1991.

[42] J. D. Hunter, "Matplotlib: A 2D graphics environment," *Comput. Sci. Eng.*, vol. 9, no. 3, pp. 90–95, 2007.

JANG-HYUN PARK received the B.S., M.S., and Ph.D. degrees in electrical engineering from Korea University, Seoul, South Korea, in 1995, 1997, and 2002, respectively. He is currently a Professor with the Department of Electrical and Control System Engineering, Mokpo National University, Mokpo, South Korea. His current research interests include neurocontrol, fuzzy control, adaptive nonlinear control, robust control, and their implementations in real plants.

• • •